

Mitochondrial heterogeneity, metabolic scaling and cell death

Aryaman, Juvid; Hoitzing, Hanne; Burgstaller, Joerg P; Johnston, Iain G; Jones, Nick S

DOI:

[10.1002/bies.201700001](https://doi.org/10.1002/bies.201700001)

License:

Creative Commons: Attribution (CC BY)

Document Version

Publisher's PDF, also known as Version of record

Citation for published version (Harvard):

Aryaman, J, Hoitzing, H, Burgstaller, JP, Johnston, IG & Jones, NS 2017, 'Mitochondrial heterogeneity, metabolic scaling and cell death', *BioEssays*. <https://doi.org/10.1002/bies.201700001>

[Link to publication on Research at Birmingham portal](#)

Publisher Rights Statement:

Checked for eligibility: 19/06/2017

General rights

Unless a licence is specified above, all rights (including copyright and moral rights) in this document are retained by the authors and/or the copyright holders. The express permission of the copyright holder must be obtained for any use of this material other than for purposes permitted by law.

- Users may freely distribute the URL that is used to identify this publication.
- Users may download and/or print one copy of the publication from the University of Birmingham research portal for the purpose of private study or non-commercial research.
- User may use extracts from the document in line with the concept of 'fair dealing' under the Copyright, Designs and Patents Act 1988 (?)
- Users may not further distribute the material nor use it for the purposes of commercial gain.

Where a licence is displayed above, please note the terms and conditions of the licence govern your use of this document.

When citing, please reference the published version.

Take down policy

While the University of Birmingham exercises care and attention in making items available there are rare occasions when an item has been uploaded in error or has been deemed to be commercially or otherwise sensitive.

If you believe that this is the case for this document, please contact UBIRA@lists.bham.ac.uk providing details and we will remove access to the work immediately and investigate.

Mitochondrial heterogeneity, metabolic scaling and cell death

Juvid Aryaman¹⁾, Hanne Hoitzing¹⁾, Joerg P. Burgstaller¹⁾²⁾³⁾, Iain G. Johnston^{4)*} and Nick S. Jones^{1)*}

Heterogeneity in mitochondrial content has been previously suggested as a major contributor to cellular noise, with multiple studies indicating its direct involvement in biomedically important cellular phenomena. A recently published dataset explored the connection between mitochondrial functionality and cell physiology, where a non-linearity between mitochondrial functionality and cell size was found. Using mathematical models, we suggest that a combination of metabolic scaling and a simple model of cell death may account for these observations. However, our findings also suggest the existence of alternative competing hypotheses, such as a non-linearity between cell death and cell size. While we find that the proposed non-linear coupling between mitochondrial functionality and cell size provides a compelling alternative to previous attempts to link mitochondrial heterogeneity and cell physiology, we emphasise the need to account for alternative causal variables, including cell cycle, size, mitochondrial density and death, in future studies of mitochondrial physiology.

Keywords:

cell death; cell size; heterogeneity; metabolic scaling; mitochondria; mitochondrial membrane potential

DOI 10.1002/bies.201700001

¹⁾ Department of Mathematics, Imperial College London, London, UK

²⁾ BHF Centre for Research Excellence, National Heart and Lung Institute, Imperial College London, Hammersmith Hospital Campus, London, UK

³⁾ Institute of Animal Breeding and Genetics, University of Veterinary Medicine, Vienna, Austria

⁴⁾ School of Biosciences, University of Birmingham, Birmingham, UK

*Corresponding authors:

Iain G. Johnston

E-mail: i.johnston.1@bham.ac.uk

Nick S. Jones

E-mail: nick.jones@imperial.ac.uk



Additional supporting information may be found in the online version of this article at the publisher's web-site.

Introduction

Non-genetic heterogeneity describes observable differences between genetically identical cells, and is a fundamental observation in cell biology [1–3], with implications for important biological phenomena including development [4, 5], bacterial persistence [6], cancer malignancy and drug resistance [7]. It is becoming increasingly recognised that variability in cellular populations of mitochondria – organelles of central bioenergetic importance – is a significant source of cellular heterogeneity in eukaryotes. As indicated experimentally by Das Neves et al. [8], and theoretically by Johnston et al. [9], mitochondrial variability could be a major driver of noise in global transcription rate which, in turn, is a key contributor to the extrinsic cellular noise observed in a wide range of downstream processes [10–14]. Indeed, recent studies have suggested that variability in mitochondrial content plays a direct role in various stochastic cellular processes, such as differentiation [15, 16], cancer metastatic potential [17] and chemotherapeutic resistance [18]; metabolic heterogeneity has also been observed to underlie fluctuations in prokaryotic systems [19]. These associations underscore the importance of continuing to expand our understanding of the origins and consequences of mitochondrial heterogeneity.

The sources of mitochondrial variability are diverse. For instance, mitochondrial membrane potential ($\Delta\Psi$) is heterogeneous in both intracellular mitochondrial populations [20] and at the aggregate level between cells [8]. For intracellular mitochondrial populations, organelles with lower $\Delta\Psi$ are less likely to join the mitochondrial network and tend to be eliminated by mitophagy [20], suggesting that $\Delta\Psi$ is a measure of mitochondrial functionality. Disruption of mitochondrial fusion can also lead to intracellular heterogeneity in $\Delta\Psi$ [21]. While the precise function of mitochondrial networks is unclear [22], it is likely that a wide range of cellular functions will depend non-linearly on the degree of

mitochondrial fusion. It is therefore reasonable to speculate that cell-to-cell variability in the mitochondrial network state may have non-trivial consequences for cellular heterogeneity, for instance, via intermediates such as ATP or reactive oxygen species production.

Since mitochondria possess their own genomes, which are replicated, degraded and stochastically partitioned during cell division [23], variability in copy number and sequence of mitochondrial DNA (mtDNA) are also important sources of bioenergetic variability, most dramatically illustrated by the profound phenotypes associated with mtDNA diseases [24]. Given the existence of two co-existing mtDNA variants, and stable mean copy numbers of each species, mathematical modelling suggests that the variance in mutant load (or heteroplasmy) of mitochondrial DNA inevitably increases over time [25]. Thus, given the existence of more than one mtDNA variant, mtDNA heteroplasmy is also a contributor to mitochondrial variability.

Recent work by Miettinen and Björklund [26] has generated a rich dataset probing the relationship between mitochondrial functionality and cell size, as an additional axis of cellular heterogeneity. The authors also explore the connection with other cellular features such as apoptosis, cell cycle and metabolism. In this paper, we consider a set of quantitative arguments that could account for this dataset. We invoke several models for bioenergetic scaling, the dynamics of cell proliferation and death, and the coupling between cell physiology and mitochondrial content. Amongst the insights gained from these models, we find that:

- Cell size scaling of cellular power demand may explain the observed reduction in mitochondrial functionality with increasing cell size, in large cells;
- The cell's characteristic (or 'optimal') size may be largely set by a particular form of intrinsic cell growth dynamics, rather than mitochondrial functionality;
- Cell death alone may be used to explain the observed non-linearity in mitochondrial functionality with cell size, if mitochondrial functionality is considered a passive indicator of the health of a cell;
- A non-heritable, non-linear relationship between mitochondrial functionality and cell size, as illustrated by Miettinen and Björklund, is compatible with a wider set of single-cell data [8] and provides a compelling alternative to link mitochondrial heterogeneity and cell physiology.

By demonstrating the existence of multiple competing hypotheses which may account for the data of Miettinen and Björklund [26], we highlight the importance of considering variables such as cell cycle, volume, mitochondrial density and cell death in future studies of mitochondrial heterogeneity. We propose further experiments to distinguish these models and further elucidate the coupling between mitochondria and cell dynamics.

Linking mitochondrial heterogeneity and cell size

Mitochondrial membrane potential is often considered a measure of mitochondrial functionality, since a higher

membrane potential may support a larger respiratory rate and ATP/ADP ratio [27, 28], as well as its role in quality control [20] (although this correspondence may not hold under all conditions, since inhibiting ATP synthase can cause membrane potential to increase [28, 29]). It is important to distinguish between total $\Delta\Psi$, which is expected to scale with a characteristic size of the system (e.g. the size of the mitochondrial population, total cellular protein or some measure of the size of the cell itself, e.g. the radius), and a measure of $\Delta\Psi$ which is normalised to account for this scaling. We denote a relative measure of $\Delta\Psi$ with $r\Delta\Psi_m$, $r\Delta\Psi_p$ or $r\Delta\Psi_r$ for normalisations by mitochondrial mass, total cellular protein and cell radius, respectively.

The main probe which Miettinen and Björklund [26] used for normalising $\Delta\Psi$ was the lipophilic cationic dye JC-1 [30]. JC-1 can pass cellular membranes and accumulates in regions of negative potential, such as the mitochondrial matrix. JC-1 is green-emitting in its monomeric form; however, if its concentration exceeds a threshold value then it forms aggregates which are red-emitting [30]. By taking the ratio of red to green signals, JC-1 is considered as a semi-quantitative measure of $r\Delta\Psi_m$. Perry et al. [29] have suggested several complexities in using this probe. Since aggregates form according to threshold effects based on the concentration of monomers, JC-1 may be ill-suited to detecting subtle gradations in $\Delta\Psi$ and has been recommended to be used as a binary indicator of high/low $\Delta\Psi$. Furthermore, it has been shown that aggregate formation is sensitive to loading concentration [31], suggesting that cellular surface-to-volume ratio may have an effect on aggregation rate. This is of particular relevance to the data of Miettinen and Björklund [26] since variations in cell size are of interest. Finally, equilibration times tend to be long for JC-1, as can be seen in [26] Fig. S2E (although the qualitative observations of this particular experiment appeared to hold throughout the staining kinetics).

Despite these complexities, many of the key insights of Miettinen and Björklund [26] were reproduced with other means of normalising mitochondrial membrane potential. Throughout their experiments, the authors used flow cytometry to measure cell size using forward scatter (FSC). Calibration of FSC is important for its rigorous interpretation [32]. Upon binning cells by diameter, with bin width of ~ 100 nm, the authors found good correlation between FSC and cell radius across the binned populations. $\Delta\Psi$ was measured with TMRE (another lipophilic cationic dye) and total cellular protein content using CellTrace FarRed stain [33] which covalently binds to cytosolic proteins. The ratio of these signals yields $r\Delta\Psi_p$. The authors found that $r\Delta\Psi_p$ initially increased and subsequently decreased (henceforth referred to as 'turning behaviour') with increasing cell radius, which was qualitatively similar to $r\Delta\Psi_m$ found via JC-1 ([26] Fig. S2K, 1C). The authors also used MitoTracker Red as a measure of $\Delta\Psi$ and MitoTracker Green as a measure of mitochondrial mass ([26] Fig. 1D). Their data suggested that $r\Delta\Psi_r$ shows turning behaviour with increasing cell radius; re-analysis of these data also suggests that $r\Delta\Psi_m$ shows turning behaviour with either increasing cell radius or volume (see Supporting Information Fig. S1).

While the precise interpretation of JC-1 ratio remains somewhat unclear due to the complexities above, the empirical observation that median JC-1 monomer

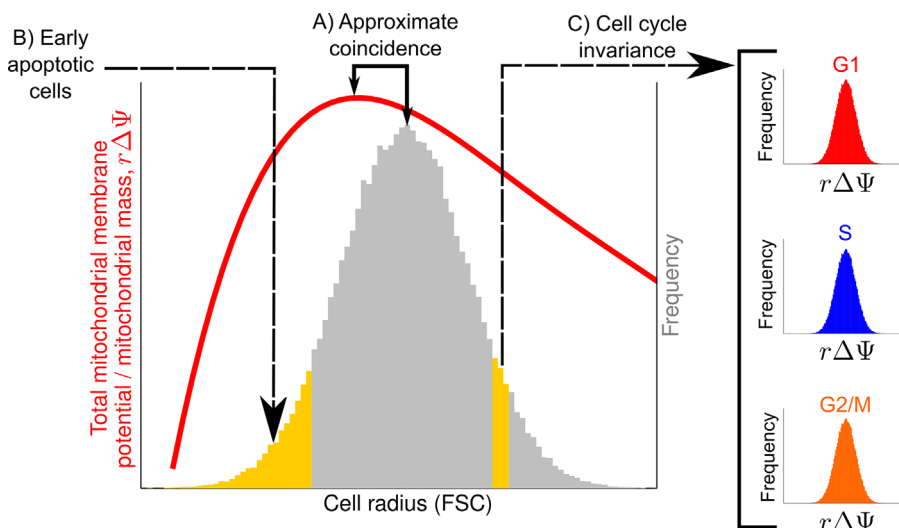


Figure 1. Summary of findings of Miettinen and Björklund. The authors binned cells by size of windows approximately 100 nm in diameter. For each bin, the authors measured total mitochondrial membrane potential, normalised by cell size, ($r\Delta\Psi$) using the ratiometric probe JC-1, and reported its median (red curve). **A:** Approximate coincidence between the mode of the cell radius distribution (grey histogram), determined through forward scatter with flow cytometry, and median $r\Delta\Psi$. **B:** Although cells were gated for cell death using propidium iodide, the smallest cells in the population were high in an alternative annexin-based sensor of cell death (pSIVA) after normalisation by cell protein content, suggesting that these were early apoptotic cells. Observations A and B do not exclusively rely on JC-1 measurements. **C:** For approximately fixed cell size, the authors showed that the distribution of $r\Delta\Psi$ was approximately invariant across different cell cycle stages (red, blue, orange histograms), suggesting that the variation in $r\Delta\Psi$ is more strongly informed by cell volume than cell cycle stage. Note that this observation was not validated independently of JC-1. Based on figures from [26].

fluorescence closely tracks median total cell protein suggests that it is appropriate for normalisation by cell size [26]. The orthogonal validation experiments suggest some degree of qualitative similarity between $r\Delta\Psi_m$, $r\Delta\Psi_p$ and $r\Delta\Psi_r$, all of which show turning behaviour with increasing cell radius. The qualitative agreement between median JC-1 ratio and these validation experiments suggest that JC-1 ratio is a qualitative measure of system-size-normalised mitochondrial membrane potential. We, therefore, use the notation $r\Delta\Psi$ to denote JC-1 measurements, which the data of [26] suggests has qualitative similarity to $r\Delta\Psi_m$, $r\Delta\Psi_p$ and $r\Delta\Psi_r$. This turning behaviour was found with the JC-1 probe in immortal cell lines from human (Jurkat), fly (Kc167) and chicken (DT40) as well as primary rat hepatocytes and human primary HUVECs (i.e. non-immortalized cells, [26] Fig. S2L), providing some evidence that this observation may hold beyond immortalized cell cultures.

Miettinen and Björklund [26] found that the maximum $r\Delta\Psi$ over cell size approximately coincided with the modal cell size – see Fig. 1. The distribution of $r\Delta\Psi$ was also invariant to cell cycle stage for cells of an approximately fixed size. The authors therefore postulated that non-linearity in

mitochondrial functionality results in an ‘optimal’ cell size [26], independently of cell cycle stage.

Cell physiological models coupled to cell death

Miettinen and Björklund speculate that an allometric decline causes reduction in mitochondrial functionality with increasing cell size [26, 34], citing the West, Brown and Enquist (WBE) model of allometric scaling of metabolism with body size [35]. Briefly, this model suggests that transport of materials through fractal space-filling networks explains the relationship between organismal mass

and metabolic activity (see Box 1 for a discussion of this hypothesis). In contrast, the authors speculate that small cells display low $r\Delta\Psi$ due to a ‘newborn effect’ whereby daughter cells inherit the low mitochondrial functionality of their parents, which itself originates from the allometric decline in the final stages of growth in parent cells. Intermediate-sized cells were postulated to ‘reset’ their metabolic activity, increasing it during early stages of growth [26, 34]. However, both the ‘newborn’ and metabolic ‘reset’ arguments suggest differences in $r\Delta\Psi$ at different stages of the cell cycle, which was not observed using JC-1 ([26] Fig. 2D, S3C and D). We note that the lack of cell-cycle dependence in $r\Delta\Psi$ was not reproduced independently of the qualitative JC-1 probe, so the newborn/reset hypothesis remains possible.

Here, we take the approach of first considering a combination of metabolic scaling and cell death as a possible link between mitochondrial behaviour and cell physiology. We will later consider an alternative purely involving cell death as the underlying causal variable of the observed non-linearity.

A bioenergetic proposal: A combination of scaling of cellular power demand with cell size, and cell death, may account for observed patterns of mitochondrial functionality

In Box 2, we propose that metabolic scaling with a particular model of cell death may recover the turning behaviour in $r\Delta\Psi$ with cell radius observed by Miettinen and Björklund [26]. The model suggests that, under non-pathophysiological circumstances, cells alter their mitochondrial functionality to maintain energy supply/demand balance at different cell volumes (v).

The model makes the non-intuitive assumption that cells do not alter their mitochondrial density in response to volume-dependent changes in cellular energy demands: one may speculate that this is due to the timescale of changes in $r\Delta\Psi$ being able to match cellular energy demands, whereas mitochondrial mass (n) may not. Proportionality between n and v has found some support in the literature [37–39]. Indeed, recent mathematical modelling [46] of the cell-physiological consequences of heteroplasmy in a deleterious

Box 1**Allometric scaling hypothesis of cellular power demands**

The WBE model of allometric scaling [35] claims that the power-law relationship linking an organism's metabolic rate (B) and mass (M) is $B \propto M^{3/4}$ and can be derived by considering the transport of materials through space-filling fractal networks of branching tubes, for instance the cardiovascular network of most vertebrates. The theory was subsequently extended to explain the metabolic requirements of single cells in terms of mitochondrial output [36]. Assuming that cell mass and volume (v) are proportional, through constant cellular density, and that the power demand (D) of a cell equates to its metabolic output, the WBE model suggests that the power demand of single cells scales as $D \propto v^{3/4}$. We model mitochondrial power supply (S) in terms of mitochondrial mass density ($\rho = n/v$, for mitochondrial mass n) and mitochondrial functionality (f) as $S \propto \rho v f$. Miettinen and Björklund [26], as well as other authors [37–39], suggest that $n \propto v$ (i.e. $\rho = \text{const}$) and therefore $S \propto v(r\Delta\Psi)$ (see Main Text for further discussion of ρ variation with v), where we have interpreted $f \propto r\Delta\Psi$. Using $S = D$ results in the prediction that $r\Delta\Psi \propto v^{-1/4}$, in contrast to the model we suggest in Equation (3).

Over the relatively small dynamic range of cell volume in a population of cells, the $r\Delta\Psi \propto v^{-1/4}$ relationship of the WBE model and Equation (3) are unlikely to make large differences in their predictions. However, there are some conceptual difficulties in accepting the WBE model above a simpler energetic scaling argument. Whilst mitochondria do form fractal-like networks [40], and the level of fusion of these networks might have non-linear effects on metabolic output [22], it is not clear that a system of static, hierarchical, tubes with fluid flow is an appropriate modelling framework to describe energy transportation within single cells. Because of this, and the criticisms sometimes levelled at allometric scaling [41–43], we have considered a scaling argument which focusses on the potential bioenergetic demands from different specific cellular compartments [44]. Nevertheless, the fusion status of the mitochondrial network remains an appealing potential explanation for the mechanism by which cells alter their mitochondrial functionality to maintain energetic homeostasis with varying cell volume. It therefore remains an interesting area of further study to quantify the extent of mitochondrial fusion and fission [45] as a function of cell volume to explain the $r\Delta\Psi$ variations observed by Miettinen and Björklund [26].

measurements) did not strongly constrain the precise relationship between n and v so other scaling relationships are feasible, see Supporting Information Section S2 for further discussion.

The scaling argument culminating in Equation (3) suggests that $r\Delta\Psi$ decreases with cell volume. This is because mitochondrial mass has been taken to scale proportionately with volume but power demands do not (Equation (1)). Small cells have lower mitochondrial mass, and must therefore have higher mitochondrial functionality to satisfy the constant component of power demand placed by, e.g. the nucleus (k_n). As cells become larger and have higher mitochondrial mass, power demand from the nucleus may be more easily satisfied, so mitochondrial functionality reduces towards a constant value k_v .

This model alone suggests that $r\Delta\Psi$ is a purely decreasing function of cell volume: however, Miettinen and Björklund observed a turning point in the relationship between $r\Delta\Psi$ and v . The data in [26] show increased cell death in the smallest cells in the population [26] (Fig. 3C), and potentially also a subtle increase in the largest cells. Furthermore, the authors observed a depolarized subpopulation of cells at low JC-1 monomer values ([26] Fig. S2G), potentially indicative of a subset of cells with low mitochondrial functionality at low cell sizes. Cell shrinkage is associated with apoptosis [48], as is loss of mitochondrial membrane potential [49]. Hence, we suggest that smaller cells have a higher cell death rate, and that mitochondrial functionality is a passive indicator of cell death under these circumstances (Fig. 2A). The result of simulating this model in a proliferating population of cells undergoing 'adder' dynamics [50, 51], whereby cells add a constant amount of volume each cell cycle, is presented in Fig. 2.

As can be seen in the distribution of cell volumes (Fig. 2C), adder dynamics imposes a characteristic cell size associated with the mode of the distribution, which is often referred to as an 'optimal' cell size. The width of the final distribution is set by the variability in partitioning of volume between daughters at division (although other sources of variability may be envisaged such as noise in the growth rate or the amount of volume added per cell cycle [54], which are neglected here). Under these simulation dynamics, the modal cell volume and the maximum value of $r\Delta\Psi$ are essentially independent (Fig. 2C) and can be tuned relatively to each other through appropriate choices of model parameters. The lack of alignment between the modal cell size and maximal $r\Delta\Psi$ could also be achieved with 'sizer' dynamics, where cells divide once exceeding a maximal cell size. The coefficient of variation (CV) in $r\Delta\Psi$ also showed a minimum (Fig. 2D), in qualitative agreement with [26], although the minimum CV was constrained to coincide with the minimum $r\Delta\Psi$ (see Supporting Information Section S4 for further discussion). It is therefore largely compatible with the data of [26] to suggest that a cell's characteristic size is set by a particular form of intrinsic cell dynamics, rather than requiring a direct link with $r\Delta\Psi$ as proposed in [26].

In Supporting Information Section S5, we explore an alternative hypothesis where cell death rate is a non-linear function of cell size, and that mitochondrial membrane potential is a passive readout of cell death rate over all values of cell volume. We found that this is also a compatible interpretation of the data presented in [26]. However, the causality of this model may also be inverted, where

mtDNA mutation associated with MELAS [47] has suggested that failure to maintain the cytoplasmic density of wild-type mitochondrial DNA is associated with a pathophysiological response in vitro. However, the data of [26] (neglecting JC-1

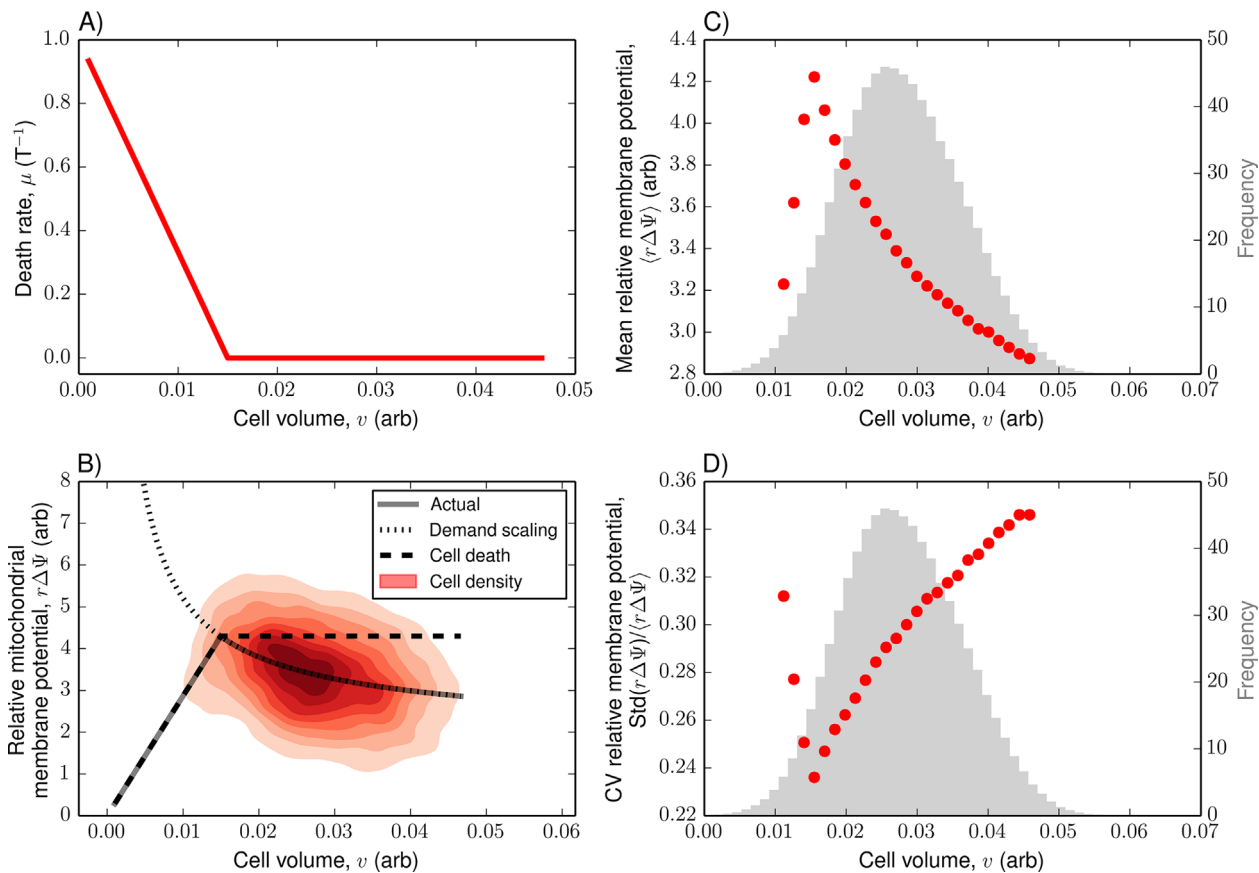


Figure 2. Power demand scaling, in conjunction with a simple cell death model, may account for observations of Miettinen et al. Cells obeying adder dynamics, initialised with random uniform volumes, were simulated with a volume-dependent death rate. **A:** Model for death rate (probability of cell death per unit of simulation time T) as a function of cell volume. Death rate was assumed to be zero after cells reach a threshold size for computational convenience. **B:** Power demand scaling (black dotted) was determined through a power supply = demand relationship in Equation (3). Cell death scaling (black dashed) was determined through a piecewise linear relationship in volume (Equation (5)). The mean $r\Delta\Psi$ (grey) was determined by taking the minimum of the demand scaling and cell death curves at every point in v (to model switching behaviour which is continuous in v). Addition of Gaussian noise to the mean relationship recovers a joint density of v and $r\Delta\Psi$ (red shaded region) similar to the findings of Miettinen and Björklund ([26] Fig. 1B). **C and D:** Cells were binned by volume in silico, and for each bin the mean and standard deviation of $r\Delta\Psi$ and v were computed. **C:** Mean $r\Delta\Psi$ (red points) shows a maximum with respect to volume which is not aligned with the modal cell volume (grey histogram of cell volumes), recapitulating the observation of Miettinen and Björklund ([26] Fig. 1C). **D:** The coefficient of variation of $r\Delta\Psi$ (red points) shows a minimum with respect to volume, as observed by Miettinen and Björklund ([26] Fig. 3A), although the location of the minimum CV and maximum average $r\Delta\Psi$ are constrained to coincide in our model (C and D) – see Supporting Information Section S4 for further discussion. For simulation details, see Supporting Information Section S3.

mitochondrial functionality is a non-linear function of cell volume, and cell death rate is linearly related to mitochondrial functionality. This interpretation aligns more closely with that of Miettinen and Björklund [26], who suggest that the

non-linearity between $r\Delta\Psi$ and v underlies their observations. This highlights the importance of excluding cell death as a potential confounding variable in future confirmatory studies so that these hypotheses may be disambiguated.

Future verification studies may include gating cells in FACS analysis based on the pSIVA cell death probe used in [26]. Alternatively, fluorescence labelling of upstream apoptosis markers, such as cytochrome-c, may allow detection of cells in early stages of cell death [55]. Combining this with fluorescence microscopy and tracking mitochondrial membrane potential, mitochondrial mass and cell volume, may allow early-apoptotic cells to be excluded and verification of the non-linearity between cell volume and relative mitochondrial membrane potential.

A parabolic function of mitochondrial functionality against cell size is compatible with a mathematical model of mitochondrial variability

A previous model, accounting for the data in [8], described the cellular consequences of mitochondrial variability in HeLa cells [9]. That model phenomenologically described mitochondrial functionality as a stochastically inherited quantity, determined through a mean-reverting process (an AR(1) process). The biological mechanism for the heritability of mitochondrial functionality was unclear from that study, although one may speculate that the inherited concentration of mitochondrial fusion proteins may be a feasible explanation for this. Indeed, recent evidence suggests that the

Box 2

Mathematical model of power demand scaling and cell death

We will relate mitochondrial functionality ($r\Delta\Psi(v)$) to cellular volume (v) by modelling $r\Delta\Psi$ as a combination of two models: the first describes the eventual decrease of $r\Delta\Psi(v)$ with v using metabolic scaling arguments, denoted by $r\Delta\Psi_s$. In contrast, the initial increasing part of $r\Delta\Psi(v)$ will be modelled using cell death arguments and denoted by $r\Delta\Psi_\mu$. A combination of $r\Delta\Psi_s$ and $r\Delta\Psi_\mu$ will be used to represent the turning behaviour observed in $r\Delta\Psi$ with cell volume and therefore also cell radius (as the two are related through a monotonic relationship).

We relate mitochondrial functionality ($r\Delta\Psi$) to cellular volume (v) by considering total cellular power supply (S) and demand (D). To represent D , we consider contributions which scale with cell volume (e.g. cytoplasmic protein content), v , surface area (e.g. work done at the plasma membrane), $v^{2/3}$, and constant terms which do not scale with cell size (e.g. replication of the genome). This may be written as

$$D = k_v v + k_s v^{2/3} + k_c \quad (1)$$

where k_i are positive real constants, which were loosely based on a study of the power demands of thymocytes [44] (see Supporting Information Section S3 for further discussion). In general, we might expect S to be of the form $S \propto v\rho(v)f(v)$, where $\rho(v)$ is mitochondrial mass density ($\rho(v) = n(v)/v$, where $n(v)$ is mitochondrial mass) and $f(v)$ is a measure of mitochondrial functionality, in an analogous form to the bioenergetic driving term in [9]. We interpret $f(v) \propto r\Delta\Psi(v)$, since larger values of $r\Delta\Psi$ support a larger respiratory rate and ATP/ADP ratio [27, 28]. We take $\rho(v) = \text{const}$ for parsimony (see Main Text for discussion). Hence,

$$S \propto v \cdot r\Delta\Psi \quad (2)$$

We model power supply as being balanced by power demand, $S = D$, with cells varying $r\Delta\Psi$ to maintain this relationship for various v . Rearrangement for $r\Delta\Psi$ yields

$$r\Delta\Psi_s(v) = k_v + k_s v^{-1/3} + k_c v^{-1} \quad (3)$$

where the subscript s denotes this metabolic scaling model for $r\Delta\Psi$.

For the cell death component of mitochondrial functionality, we assume that the cell death rate ($\mu(v)$, the probability of cell death per unit time of individual cells) increases amongst cells with smaller volumes. Above a threshold volume (determined by continuity), cell death is modelled as negligible. We then model relative membrane potential as a passive indicator of the cellular death rate μ , since cells which are apoptotic tend to have low mitochondrial membrane potential [49]. We hence use the following linear functions,

$$\mu = \begin{cases} -m_\mu v + c_\mu, & \text{if } v < \frac{c_\mu}{m_\mu} \\ 0, & \text{otherwise} \end{cases} \quad (4)$$

$$r\Delta\Psi_\mu(v) = -m_\psi \mu + c_\psi \quad (5)$$

where c_μ , c_ψ , m_μ and m_ψ are positive real constants. With this, we recover an alternative description of $r\Delta\Psi$ which initially increases with volume because $r\Delta\Psi_\mu$, μ and v are each connected by negative linear relationships.

We combine $r\Delta\Psi_s$ and $r\Delta\Psi_\mu$ through a rule which ensures continuity in $r\Delta\Psi$. For mathematical convenience, we choose $r\Delta\Psi(v) = \min\{r\Delta\Psi_s(v), r\Delta\Psi_\mu(v)\}$ for all v . This function will show a turning point as cells switch from having their membrane potential governed by risk of cell death to power demand scaling, for increasing cell size. $r\Delta\Psi$ is then observed with Gaussian noise $N(0, \sigma_\psi)$ with standard deviation (SD) σ_ψ , which accounts for technical and biological sources of noise.

We used a stochastic hybrid systems approach [52] to simulate a population of exponentially growing cells undergoing 'adder' dynamics [50, 51], whereby cells add a constant amount of volume (K_v) to their initial volume (v_0) each cell cycle, which has found recent support in bacteria [53]. Cells are modelled to then divide by stochastically partitioning their volume, with the first daughter inheriting volume $v_1 = N((v_0 + K_v)/2, \sigma_v)$ (with SD σ_v), and the second inheriting $v_2 = v_0 + K_v - v_1$ through conservation of mass. Cell death events occur stochastically according to the rate $\mu(v)$ (Equation (4)), see Supporting Information Section S3 for simulation details. The results of this model are shown in Fig. 2.

proliferation rate of yeast is heritable, and that slow-growing cells have higher oxidative stress whose proliferation rate may be rescued with an anti-oxidant, suggesting a link to mitochondrial functionality [56]. Further studies are required to determine whether this is true for a larger class of systems, including mammalian cells.

The data of Miettinen and Björklund [26] immediately suggests an alternative nonlinear relationship between function and dynamics (see Fig. 1). We hypothesised that this relationship may be sufficient to account for the data in [8]

without invoking a phenomenological mechanism for the stochastic inheritance of mitochondrial functionality (though the stochastic inheritance of mitochondrial mass remains supported). Briefly, the model of Johnston et al. [9] predicts the relationship between cell volume, mitochondrial content and mitochondrial functionality with a pair of coupled ordinary differential equations. Cells undergo sizer dynamics, and the population size is controlled to be static over time.

Here, we replace the stochastic inheritance of mitochondrial functionality by approximating the result of Miettinen

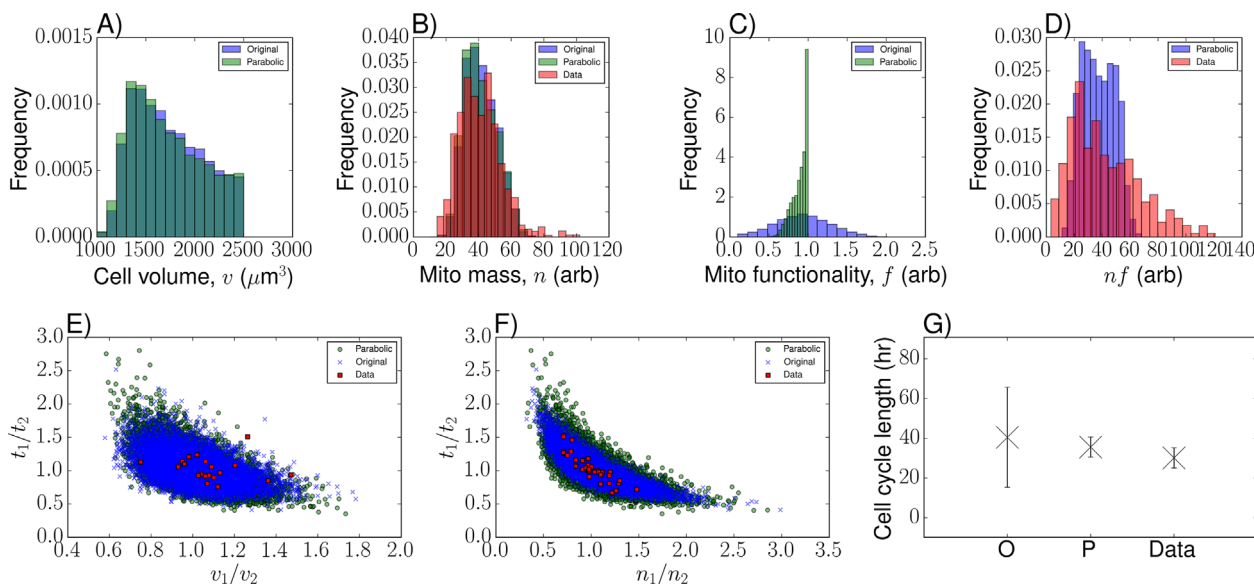


Figure 3. Nonlinear connection between mitochondrial functionality and cell volume is consonant with a wider set of single cell data. Replacing the stochastic process determining mitochondrial functionality (Original) with the parabolic relationship in Equation (6) (Parabolic), and comparisons with data from [8] where available. **A:** Distribution of cell volumes is relatively unchanged by the modification of f . **B:** Distribution of mitochondrial mass in both models are comparable with data. **C:** Distribution of mitochondrial functionality. Since Equation (6) is deterministic, f cannot exceed its maximal value f_{\max} , causing the skewness observed. **D:** The distribution of total mitochondrial functionality nf has a reduced variance in the parabolic model, which departs somewhat from the data of [8]. **E:** Relationship between ratio of cellular volumes at birth and the ratio of cell cycle lengths for sister pairs. **F:** Relationship between ratio of mitochondrial contents at birth and the ratio of cell cycle lengths for sister pairs. Both models are comparable with data in E and F. **G:** Mean cell cycle lengths \pm standard deviation for the original (O) and parabolic (P) models, as well as the experimental observation in [8] (Data). The variance in cell cycle lengths is greatly reduced, since an additional source of variability is removed in P from the deterministic relationship Equation (6), which has better agreement with data. $v_{\text{opt}} = 2000$, $f_m = 2.0$, $f_{\max} = 1.0$. All other parameters appearing in the original model were kept the same as [9].

and Björklund as a non-heritable parabolic relationship between mitochondrial functionality (which we interpret as $r\Delta\Psi$) and cell volume v

$$r\Delta\Psi \propto f = f_{\max} - f_m \left(\frac{v - v_{\text{opt}}}{v_{\text{opt}}} \right)^2 \quad (6)$$

where f_{\max} is the peak value of f , occurring when $v = v_{\text{opt}}$, and f_m is the steepness of the parabola. In implementing the original model from [9], it was found that constraining $f > 0.1$ from the AR(1) process (rather than $f > 0.01$ described in [9]) yielded a better comparison to experimental cell cycle lengths. The result of replacing the AR(1) process in [9] with the deterministic relationship in Equation (6) is shown in Fig. 3.

We found that whilst the distributions of cell volume and mitochondrial mass were relatively unchanged (Fig. 3A and B), mitochondrial functionality had greater skewness under the

parabolic model (Fig. 3C). The distribution of total mitochondrial content nf was narrower in the parabolic model (SD = 11.5) than the original model (SD = 17.4) (Fig. 3D) which has poorer agreement with data from [8]. However, the cell cycle length distribution in the parabolic model had much better agreement in its standard deviation (SD = 5.07) than the original model (SD = 25.2) compared with data (SD = 5.13) (Fig. 3H). The low degree of correlation between cell cycle lengths between parent and daughter cells was also retained (Original: $R^2 = 0.11$, Parabolic: $R^2 = 0.05$) in agreement with the data of [8] (Fig. 3C of [9]). Overall, this shows that the non-heritable non-linear mechanism between mitochondrial functionality and cell volume found in [26] may broadly account for the data in [8] without invoking a phenomenological stochastic model for the inheritance of mitochondrial functionality.

Conclusion

Heterogeneity in mitochondrial content is exerted along many axes, including intrinsic functional variability, network status and genetic variability. A host of cellular phenomena are affected by noise, a growing number of which are being directly attributed to mitochondrial variability. The study of Miettinen and Björklund [26] has extended this picture by probing the link between mitochondrial content and cell volume, suggesting a non-linear relationship between mitochondrial functionality and cell radius.

We have shown that a simple model of power demand scaling predicts a decreasing trend in relative mitochondrial functionality with increasing cell volume. By combining this with a simple cell death model, we were able to qualitatively account for a large number of observations by Miettinen and Björklund [26]. We also found that incorporating the nonlinear relationship between $r\Delta\Psi$ and cell volume as suggested by Miettinen and Björklund into a model of mitochondrial heterogeneity [9] was broadly consonant with a wider set of single cell data [8]. We have found that it is also compatible with the data of [26] to suggest that cell death is the causal

variable in determining the non-linearity in $r\Delta\Psi$. Our analysis has shown the existence of multiple competing hypotheses which are able to account for the data of Miettinen and Björklund, thus highlighting the importance of accounting for cell cycle, volume, mitochondrial density and cell death in future single-cell studies of mitochondrial heterogeneity.

Acknowledgments

We would like to thank Teemu Miettinen and Markus Schwarzländer for their helpful discussions and comments on the manuscript. We would also like to thank Tristan Rodriguez for advice on experimental suggestions.

The authors have declared no conflicts of interest.

References

1. Elowitz MB, Levine AJ, Siggia ED, Swain PS. 2002. Stochastic gene expression in a single cell. *Science* **297**: 1183–6.
2. Swain PS, Elowitz MB, Siggia ED. 2002. Intrinsic and extrinsic contributions to stochasticity in gene expression. *Proc Natl Acad Sci USA* **99**: 12795–800.
3. Raj A, van Oudenaarden A. 2008. Nature, nurture, or chance: stochastic gene expression and its consequences. *Cell* **135**: 216–26.
4. Vassar R, Ngai J, Axel R. 1993. Spatial segregation of odorant receptor expression in the mammalian olfactory epithelium. *Cell* **74**: 309–18.
5. Chang HH, Hemberg M, Barahona M, Ingber DE, et al. 2008. Transcriptome-wide noise controls lineage choice in mammalian progenitor cells. *Nature* **453**: 544–7.
6. Kussell E, Kishony R, Balaban NQ, Leibler S. 2005. Bacterial persistence. *Genetics* **169**: 1807–14.
7. Brock A, Chang H, Huang S. 2009. Non-genetic heterogeneity—a mutation-independent driving force for the somatic evolution of tumours. *Nat Rev Genet* **10**: 336–42.
8. Das Neves RP, Jones NS, Andreu L, Gupta R, et al. 2010. Connecting variability in global transcription rate to mitochondrial variability. *PLoS Biol* **8**: e1000560.
9. Johnston IG, Gaal B, Das Neves RP, Enver T, et al. 2012. Mitochondrial variability as a source of extrinsic cellular noise. *PLoS Comput Biol* **8**: 1–14.
10. Ross IL, Browne CM, Hume DA. 1994. Transcription of individual genes in eukaryotic cells occurs randomly and infrequently. *Immunol Cell Biol* **72**: 177–185.
11. Blake WJ, Kærn M, Cantor CR, Collins JJ. 2003. Noise in eukaryotic gene expression. *Nature* **422**: 633–7.
12. Newman JR, Ghaemmaghami S, Ihmels J, Breslow DK, et al. 2006. Single-cell proteomic analysis of *S. cerevisiae* reveals the architecture of biological noise. *Nature* **441**: 840–6.
13. Volfson D, Marciniak J, Blake WJ, Ostroff N, et al. 2006. Origins of extrinsic variability in eukaryotic gene expression. *Nature* **439**: 861–4.
14. Bar-Even A, Paulsson J, Maheshri N, Carmi M, et al. 2006. Noise in protein expression scales with natural protein abundance. *Nat Genet* **38**: 636–43.
15. Katajisto P, Döhla J, Chaffer CL, Pentimikko N, et al. 2015. Asymmetric apportioning of aged mitochondria between daughter cells is required for stemness. *Science* **348**: 340–3.
16. Sukumar M, Liu J, Mehta GU, Patel SJ, et al. 2016. Mitochondrial membrane potential identifies cells with enhanced stemness for cellular therapy. *Cell Metab* **23**: 63–76.
17. LeBleu VS, O'Connell JT, Herrero KNG, Wikman H, et al. 2014. PGC-1 α mediates mitochondrial biogenesis and oxidative phosphorylation in cancer cells to promote metastasis. *Nat Cell Biol* **16**: 992–1003.
18. Lee DG, Choi BK, Kim YH, Oh HS, et al. 2016. The repopulating cancer cells in melanoma are characterized by increased mitochondrial membrane potential. *Cancer Lett* **382**: 186–94.
19. Kiviet DJ, Nghe P, Walker N, Boulineau S, et al. 2014. Stochasticity of metabolism and growth at the single-cell level. *Nature* **514**: 376–9.
20. Twigg G, Elorza A, Molina AJ, Mohamed H, et al. 2008. Fission and selective fusion govern mitochondrial segregation and elimination by autophagy. *EMBO J* **27**: 433–46.
21. Chen H, Chomyn A, Chan DC. 2005. Disruption of fusion results in mitochondrial heterogeneity and dysfunction. *J Biol Chem* **280**: 26185–92.
22. Hoitzing H, Johnston IG, Jones NS. 2015. What is the function of mitochondrial networks? A theoretical assessment of hypotheses and proposal for future research. *BioEssays* **37**: 687–700.
23. Johnston IG, Jones NS. 2015. Closed-form stochastic solutions for non-equilibrium dynamics and inheritance of cellular components over many cell divisions. In *Proc. R. Soc. A, The Royal Society*, volume 471, 20150050.
24. Taylor R, Turnbull D. 2005. Mitochondrial DNA mutations in human disease. *Nat Rev Genet* **6**: 389.
25. Johnston IG, Jones NS. 2016. Evolution of cell-to-cell variability in stochastic, controlled, heteroplasmic mtDNA populations. *Am J Hum Genet* **99**: 1150–62.
26. Miettinen P, Björklund M. 2016. Cellular allometry of mitochondrial functionality establishes the optimal cell size. *Dev Cell* **39**: 370–82.
27. Nicholls DG. 1977. The effective proton conductance of the inner membrane of mitochondria from brown adipose tissue. *Eur J Biochem* **77**: 349–56.
28. Nicholls DG. 2004. Mitochondrial membrane potential and aging. *Aging Cell* **3**: 35–40.
29. Perry SW, Norman JP, Barbieri J, Brown EB, et al. 2011. Mitochondrial membrane potential probes and the proton gradient: a practical usage guide. *Biotechniques* **50**: 98.
30. Smiley ST, Reers M, Mottola-Hartshorn C, Lin M, et al. 1991. Intracellular heterogeneity in mitochondrial membrane potentials revealed by a J-aggregate-forming lipophilic cation JC-1. *Proc Natl Acad Sci USA* **88**: 3671–5.
31. Mathur A, Hong Y, Kemp BK, Barrientos AA, et al. 2000. Evaluation of fluorescent dyes for the detection of mitochondrial membrane potential changes in cultured cardiomyocytes. *Cardiovasc Res* **46**: 126–38.
32. Tzur A, Moore JK, Jorgensen P, Shapiro HM, et al. 2011. Optimizing optical flow cytometry for cell volume-based sorting and analysis. *PLoS ONE* **6**: e16053.
33. Zhou W, Kang HC, O'Grady M, Chambers KM, et al. 2016. CellTrace™ Far Red & CellTracker™ Deep Red—long term live cell tracking for flow cytometry and fluorescence microscopy. *J Biol Methods* **3**: e38.
34. Miettinen TP, Björklund M. 2017. Mitochondrial function and cell size: an allometric relationship. *Trends Cell Biol*, in press, <https://doi.org/10.1016/j.tcb.2017.02.006>
35. West GB, Brown JH, Enquist BJ. 1997. A general model for the origin of allometric scaling laws in biology. *Science* **276**: 122–6.
36. West GB, Woodruff WH, Brown JH. 2002. Allometric scaling of metabolic rate from molecules and mitochondria to cells and mammals. *Proc Natl Acad Sci USA* **99**: 2473–8.
37. Posakony JW, England JM, Attardi G. 1977. Mitochondrial growth and division during the cell cycle in HeLa cells. *J Cell Biol* **74**: 468–91.
38. Rafelski SM, Viana MP, Zhang Y, Chan YHM, et al. 2012. Mitochondrial network size scaling in budding yeast. *Science* **338**: 822–4.
39. Jajoo R, Jung Y, Huh D, Viana MP, et al. 2016. Accurate concentration control of mitochondria and nucleoids. *Science* **351**: 169–72.
40. Aon MA, Cortassa S, O'Rourke B. 2004. Percolation and criticality in a mitochondrial network. *Proc Natl Acad Sci USA* **101**: 4447–52.
41. Darveau CA, Suarez RK, Andrews RD, Hochachka PW. 2002. Allometric cascade as a unifying principle of body mass effects on metabolism. *Nature* **417**: 166–70.
42. Savage VM, Deeds EJ, Fontana W. 2008. Sizing up allometric scaling theory. *PLoS Comput Biol* **4**: e1000171.
43. Kolokotronis T, Savage V, Deeds EJ, Fontana W. 2010. Curvature in metabolic scaling. *Nature* **464**: 753–6.
44. Buttgerit F, Brand MD. 1995. A hierarchy of ATP-consuming processes in mammalian cells. *Biochem J* **312**: 163–7.
45. Sukhorukov VM, Dikov D, Reichert AS, Meyer-Hermann M. 2012. Emergence of the mitochondrial reticulum from fission and fusion dynamics. *PLoS Comput Biol* **8**: e1002745.
46. Aryaman J, Johnston IG, Jones NS. 2016. Mitochondrial DNA density homeostasis accounts for the threshold effect in human mitochondrial disease. [doi:10.1101/078519](https://doi.org/10.1101/078519). *bioRxiv* 078519.
47. Picard M, Zhang J, Hancock S, Derbeneva O, et al. 2014. Progressive increase in mtDNA 3243A>G heteroplasmy causes abrupt transcriptional reprogramming. *Proc Natl Acad Sci USA* **111**: E4033–42.
48. Kerr JF, Wyllie AH, Currie AR. 1972. Apoptosis: a basic biological phenomenon with wide-ranging implications in tissue kinetics. *Br J Cancer* **26**: 239.
49. Gottlieb E, Armour S, Harris M, Thompson C. 2003. Mitochondrial membrane potential regulates matrix configuration and cytochrome c release during apoptosis. *Cell Death Differ* **10**: 709–17.

50. **Sompayrac L, Maaløe O.** 1973. Autorepressor model for control of DNA replication. *Nature* **241**: 133–5.
51. **Amir A.** 2014. Cell size regulation in bacteria. *Phys Rev Lett* **112**: 208102.
52. **Vargas-Garcia CA, Soltani M, Singh A.** 2016. Conditions for cell size homeostasis: a stochastic hybrid systems approach. *IEEE Life Sci Lett.*
53. **Taheri-Araghi S, Bradde S, Sauls JT, Hill NS,** et al. 2015. Cell-size control and homeostasis in bacteria. *Curr Biol* **25**: 385–91.
54. **Modi SK, Vargas-Garcia CA, Ghusinga KR, Singh A.** 2016. Analysis of noise mechanisms in cell size control. biorxiv: 080465. *bioRxiv* 080465.
55. **Otera H, Miyata N, Kuge O, Mihara K.** 2016. Drp1-dependent mitochondrial fission via MiD49/51 is essential for apoptotic cristae remodeling. *J Cell Biol* **212**: 531–44.
56. **Van Dijk D, Dhar R, Missarova AM, Espinar L,** et al. 2015. Slow-growing cells within isogenic populations have increased RNA polymerase error rates and DNA damage. *Nat Commun* **6**: 7972.